Signature of the coronal hole near the north crest equatorial anomaly over Egypt during the strong geomagnetic storm 5 April 2010

A. Shimeis,[1,2] I. Fathy,[1,2] C. Amory-Mazaudier,[2] R. Fleury,[3] A. M. Mahrous,[1] K. Yumoto,[4,5] and K. Groves[6]

[1]   In this paper we study the ionospheric–magnetic disturbance during a strong magnetic storm on 5 April 2010 associated to a coronal hole. The Earth was under the influence of a high speed solar wind stream during four days, and IMF was southward during a very long period. The variation of the disturbed magnetic observations and GPS-TEC are compared with the variation of quiet days during the same month in order to obtain the characteristics of GPS-TEC and magnetic disturbances due to the coronal hole effect. We use multi-instruments as SCINDA-GPS station at Helwan, Egypt (29.86°N, 31.32°E) and ASW-MAGDAS station at Aswan, Egypt (23.59°N, 32.51°E) in the equatorial region. At the beginning of the storm our data highlights the effect of the prompt penetration of the magnetosphere electric field which strongly increases the TEC. During the recovery phase of the storm, we observe on TEC and magnetic data, the signature of the ionospheric disturbance dynamo due to wind produced by Joule heating in the auroral zone. It is the first time that we observe an anti-Sq circulation on magnetic data during four consecutive days associated to the high speed solar wind streams.

1.   Introduction

[2]   In this paper we analyze the low latitude ionospheric-geomagnetic signature of the solar event of April 2010. This event was previously studied by *Möstl et al.* [2010] who described in detail the shock associated with the coronal mass ejection of 3 April 2010 and by *Connors et al.* [2011] who analyzed the magnetic flux transfer event associated to the impact of the shock on the magnetosphere on 5 April 2010 at 08:25 UT. We will focus our attention on the low latitude ionospheric and geomagnetic disturbance observed at the crest of ionization of the northern hemisphere in Africa. We analyzed the signature of the high speed solar wind stream flowing from the coronal hole which follows the CME.

[3]   During storms, at low latitudes, the ionospheric disturbances and their associated magnetic disturbances are mainly due to the intensification of the auroral electrojets. The auroral currents affect the ionospheric electric fields and currents and the thermospheric circulation on a global scale. Two main physical processes are well known: the prompt penetration of the magnetospheric convection electric field [*Vasyliunas*, 1970] and the Ionospheric disturbance dynamo [*Blanc and Richmond*, 1980].

[4]   The prompt penetration of magnetospheric convection affects simultaneously high and low latitudes and was interpreted by *Nishida et al.* [1966] as the transmission of the magnetospheric convection electric field from high to low latitudes. The magnetic disturbance associated to this physical process was named DP_2 by *Nishida* [1968]. Many experimental and theoretical studies of the prompt penetration of magnetospheric convection were made during the last decades [*Vasyliunas*, 1970; *Senior and Blanc*, 1984; *Mazaudier*, 1985; *Spiro et al.*, 1988; *Kikuchi et al.*,1996; *Kobéa et al.*, 1998, 2000; *Peymirat et al.* 2000; *Mene et al.*, 2011].

[5]   The auroral electrojets currents also transfer thermal energy to the neutral gas via Joule heating and impulses through the ion-neutral momentum transfer. This process sets up gravity waves and equatorward thermospheric winds (Hadley cell between the poles and the equator) at F region

---
[1]Space Weather Center, Faculty of Science, Helwan University, Helwan, Egypt.
[2]LPP/CNRS/UPMC, UMR 7648, Saint-Maur-des-Fossés, France.
[3]National School of Telecommunications of Brest, Brest, France.
[4]Department of Earth and Planetary Sciences, Kyushu University, Fukuoka, Japan.
[5]Space Environment Research Center, Kyushu University, Fukuoka, Japan.
[6]Air Force Research Laboratory, Hanscom AFB, Massachusetts, USA.

Corresponding author: C. Amory-Mazaudier, LPP/CNRS/UPMC, UMR 7648, 4 Av. de Neptune, Saint-Maur-des-Fossés F- 94107, France. (christine.amory@lpp.polytechnique.fr)

Table 1. Daily Value of the Am Index From 3 to 10 April 2010

Period	3 April	4 April	5 April	6 April	7 April	8 April	9 April	10 April
⟨Am⟩	16 quiet	25	64	60	38	21	10	5 quiet

altitudes [*Testud and Vasseur*, 1969; *Richmond and Matshushita*, 1975; *Richmond and Roble*, 1979]. These winds extend from auroral zone to mid and low latitudes [*Mazaudier and Bernard*, 1985; *Mazaudier et al.*, 1985] with a small return flow at the *E* region altitudes around the equator (below about 120 km altitude). *Blanc and Richmond* [1980] proposed the physical process of the ionospheric disturbance dynamo delayed after the storm. *Le Huy and Amory-Mazaudier* [2005, 2008] isolated the magnetic disturbance due to this physical process and named it Ddyn. During the last decades many experimental and theoretical studies illustrated the characteristics of to the ionospheric disturbance dynamo process [*Fejer et al.*, 1983; *Sastri*, 1988; *Abdu et al.*, 1997; *Fambitakoye et al.*, 1990; *Mazaudier and Venkateswaran*, 1990; *Fejer and Scherliess*, 1995; *Richmond et al.*, 2003; *Zaka et al.*, 2009, 2010a, 2010b]. The storm winds also lift the ionization to regions of lower loss, producing daytime increases in hmF2, in foF2, and in total electron content (TEC) and global changes in the atmospheric composition [*Jones*, 1971; *Jones and Rishbeth*, 1971; *Volland*, 1979].

[6] In this paper we analyze the low latitude ionospheric-magnetic disturbance associated with a solar coronal hole. Section 2 describes the data sample and the data processing. Section 3 presents the data analysis and data interpretation. Section 4 is devoted to the discussion and the conclusion. This work is developed in the framework of the International Space Weather Initiative project (www.iswi-secretariat.org).

2. Data Sets and Data Processing

[7] During the strong geomagnetic storm of 5 April 2010 at the beginning of sunspot solar cycle 24, a coronal hole was observed by SOHO Extreme UV Telescope after the CME of 3 April 2010 which reached the Earth on 5 April 2010. We analyze the whole period from 3 to 10 April 2010 which included a magnetic quiet period before and after the storm.

2.1. Data Sets

[8] To study the ionospheric-magnetic signature of this event we used the following primary parameters:

[9] 1. Satellite data from SOHO to determine the existence of coronal hole (http://spaceweather.com/images2010/03apr10/coronalhole_soho_blank.gif?PHPSESSID=7rdbb91a85aujvfn9gf5smps55).

[10] 2. Vx and IMF Bz recorded on board the satellite ACE (http://www.srl.caltech.edu/ACE/ASC/browse/view_browse_data.html), in order to know the convection Ey electric field.

[11] 3. Magnetic indices Dst, AU and AL from Data Analysis Center for Geomagnetism and Space Magnetism Graduate School of Science, Kyoto University website (http://wdc.kugi.kyoto-u.ac.jp/wdc/Sec3.html), to approach magnetospheric and auroral electric currents.

[12] 4. Am magnetic indices to select magnetic quiet days [*Mayaud*, 1980; *Menvielle et al.*, 2009]. The criterion for the selection of a magnetic quiet day is that the daily average ⟨Am⟩ is smaller than 20 nT. Table 1 gives the value of the Am index for the analyzed period.

[13] 5. Raw data of the Total Electron Content from the Helwan GPS SCINDA station.

[14] 6. Raw data of the Earth's magnetic field from the Aswan MAGDAS station.

[15] Table 2 gives the geographic and geomagnetic coordinates of the two ground level stations, of Helwan and Aswan, located in Egypt, which are part: the GPS SCINDA network and the MAGDAS network of magnetometers.

[16] The Scintillation Network and Decision Aid (SCINDA) is a network of ground based receivers that monitors scintillations at the UHF and L band frequencies caused by electron density irregularities in the equatorial ionosphere [*Groves et al.*, 1997].

[17] The PI of MAGnetic Data Acquisition System (MAGDAS) project due to Prof. K. Yumoto, (Space Environment Research Center, SERC, Kyushu University, Fukuoka, Japan) seeks to deploy around the world in a strategic fashion a new generation of tri-axial fluxgate magnetometers which transfer the digitized data to a central SERC server in real-time for space weather study and application during the IHY period (2007–2009). The strategy is to put the magnetometers in well-defined "bands" on the globe that are useful for scientific exploration [*Maeda and Yumoto*, 2009].

2.2. Data Processing

[18] To analyze this event we calculate secondary parameters from the primary ones listed above:

[19] 1. The convection electric field

$$IEF = -V_X B_Z.$$

[20] 2. The mean averaged quiet TEC: ⟨TEC⟩ computed as the mean arithmetic value of the most magnetic quietest days of April 2010 (Table 3 gives the Am value of the quietest days of April) $\langle vTECquiet \rangle = \frac{1}{n} \sum_{i=1}^{n} (vTECquiet)i$, where i equal 1,…6: there is no data on 30 April.

[21] 3. The mean averaged quiet ΔH component of the Earth's magnetic field at Aswan, computed as the mean

Table 2. Geographic and Geomagnetic Coordinates of the Two Stations of Helwan and Aswan in Egypt

Station Name	Geographic Latitude (N)	Geographic Longitude (E)	Geomagnetic Latitude	Geomagnetic Longitude	Install
Helwan	29.50	31.20	21.44	102.70	11/2009
Aswan	23.59	32.51	15.20	104.24	23/12/2008

Table 3. List of the Most Magnetic Quiet Days of April 2010 Determined With the Am Indices

Quiet Days	i=1 13 April	i=2 16 April	i=3 18 April	i=4 25 April	i=5 26 April	i=6 28 April	i=7 30 April
Daily⟨Am⟩	4	4	2	3	2	4	4

averaged TEC$\langle \Delta H quiet \rangle = \frac{1}{n} \sum_{i=1}^{n} (\Delta H quiet)i$, where i equal 1,...7.

[22] 4. The ionospheric electric current disturbance Diono. The observed ΔH variation is the sum of 2 terms: $\Delta H = S_r + D$.

[23] S_R is the daily regular variation of the Earth's magnetic field due to the regular electric current associated with winds driven by the solar heating and D is the disturbed variation due to the electric currents generated by disturbances. The irregular component D of the magnetic field is the sum of the effects of various current systems of the Earth's environment [Cole, 1966; Fukushima and Kamide, 1973]:

$$D = Diono + DR + DCF + DT + DG$$

Diono is the magnetic effects of the disturbed ionospheric electric current systems flowing mainly in the E region and generated by disturbance processes: the direct penetration of the magnetospheric convection electric field and the ionospheric disturbance dynamo;

[24] DG stands for the effects of induced currents which have similar variations than the external current with a smaller amplitude ∼qq% [Sabaka et al., 2004]. In a first approach we neglect them.

[25] DCF and DT are the Chapman Ferraro currents and tail currents. During the recovery phase, the ring current DR is the stronger one and we can neglect the disturbance of the Chapman Ferraro currents (DCF) and tail current (DT).

[26] Therefore, during the recovery phase D reduces to $D = DR + Diono$.

[27] DR is the disturbance mainly due to ring current, we can estimate DR by using the Dst magnetic index: $DR = Dst. \cos(\lambda)$, where λ is the co-latitude (90 - geographic latitude) of the station.

[28] Diono is composed of several terms: Diono = $DP_2 + D_{dyn} + DP_1$.

[29] DP_2 is the equivalent current system related to the prompt penetration of the magnetospheric convection electric field [Nishida, 1968], D_{dyn} is the equivalent current system related to the ionospheric disturbance dynamo process [Le Huy and Amory-Mazaudier, 2005, 2008] and DP_1 is the equivalent current system related to substorm event acting on the nightside [Rostoker, 1969].

[30] Following all these considerations: The ΔH component expression becomes Δ, and the magnetic disturbance Diono is $Diono = H - Dst*\cos(\lambda) - S_R$.

[31] To evaluate the regular variation S_R we used the quietest days of the month:

$$\langle \Delta H quiet \rangle = \frac{1}{n} \sum_{i=1}^{n} (\Delta H quiet)i.$$

## 3. Data Analysis, Results and Discussion

3.1. Data Analysis

[32] In this paper we present the low latitudes ionospheric and geomagnetic effects of the storm on 5 April 2010 related to the shock associated with the coronal mass ejection of 3 April 2010. The SSC was detected near the Earth on 5 April 2010 at 08.25. The CME was followed by high speed solar wind streams flowing from a solar coronal hole observed with the SOHO satellite from 3 to 10 April. This coronal hole is shown in Figure 1. We analyze the period from 3 to 10 April including the magnetic quiet period preceding the storm, the whole recovery phase of the storm and the magnetic quiet period following the storm.

[33] Figure 2 illustrates the time variation of the solar wind, interplanetary magnetic field and geomagnetic indices during the selected period. Figure 2 is composed of four panels: the x component of the solar wind Vx with a time resolution of 1 min (Figure 2a), the z component of the interplanetary magnetic field Bz with a time minute of 5 min (Figure 2b). Figures 2c and 2d are devoted respectively to the Dst magnetic index (Figure 2c) and AU and AL indices. The time resolution is one minute for all these magnetic indices.

[34] On 5 April, Vx (Figure 2a) increased from 500 km/s to 700 km/sec at the time of the SSC and reached the maximum value at 800 km/sec on 13:00 UT. It remained at 600 km/sec (on the average) from 6 to 8 April 2010. Vx started to decrease around 18:00 UT on 8 April 2010, to reach 450 km/s on 9 April around 12:00UT, and increased again until 500 km/s at around 00:00 UT on 10 April 2010.

[35] The IMF Bz (Figure 2b) turned southward at around 08:26 UT on 5 April and reached the maximum value of
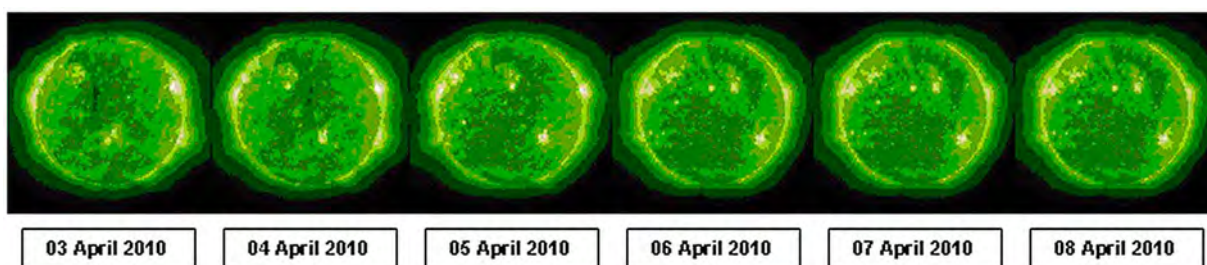
Figure 1. Coronal hole observed by SOHO.
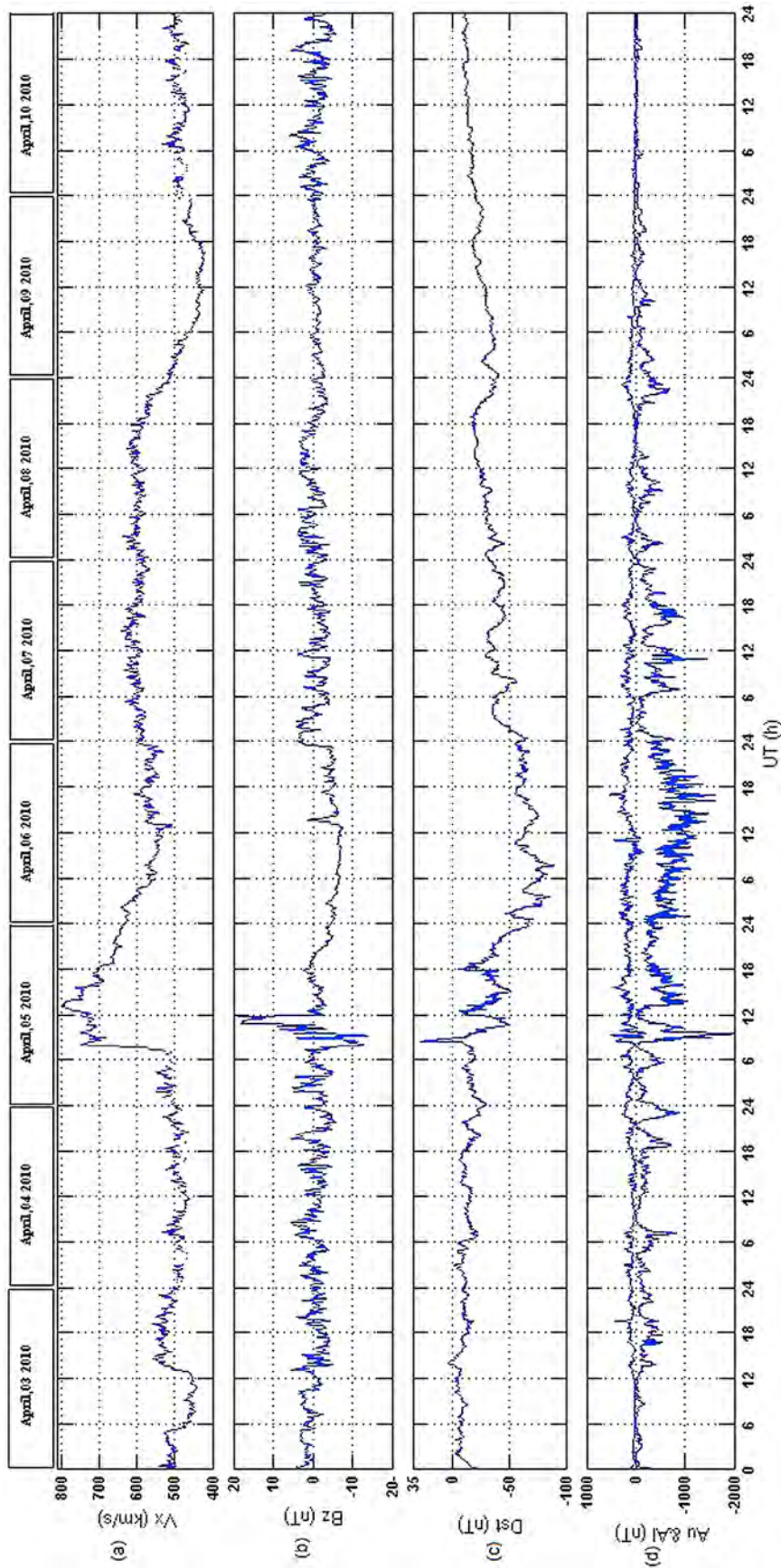
Figure 2. The solar wind parameters and geomagnetic indices for strong storm from 3 to 10 April 2010: (a) component Vx of the solar wind speed, (b) the Bz component of the interplanetary magnetic field, (c and d) the Dst index and the AU and AL indices.
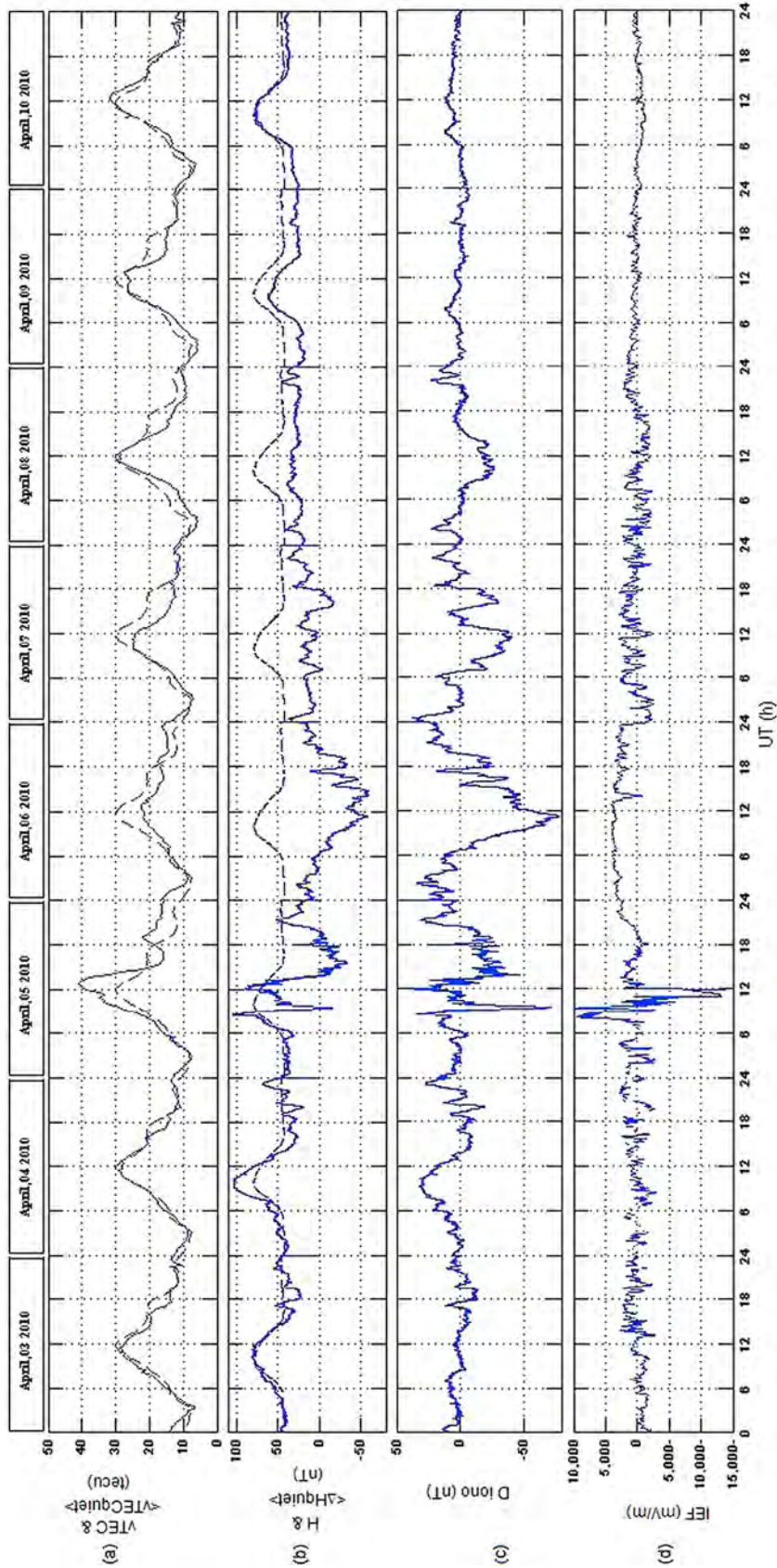
Figure 3. The daily variations for the whole period: (a) vertical total electron content (vTEC), (b) horizontal component of Earth's magnetic field (H) where the dashed curve for most quiet days (sunspot number (Am) ≤4), (c and d) ionospheric disturbance (Diono) and interplanetary electric field (IEF).

−19 nT. It remained negative for several hours until 10:30UT on 5 April 2010, except for several northward excursions until 11:00 UT on 5 April 2010. IMF Bz turned southward again around 11:00 UT and remained negative for one day (long time duration) on 6 April 2010, except a round 13:00UT: it exhibits a northward peak. IMF Bz returned to its values before the storm at 03:00UT on 7 April 2010.

[36] The Dst index (Figure 2c) increased strongly from −10nT to 35 nT at the time of SSC. Then it decreased and had two negative peaks excursions of the same amplitude −50 nT around 11:00 and at14:00 UT during the main phase of the storm on 5 April 2010. The Dst reached the minimum value of −100nT around 12:00 UT on 6 April 2010. Dst returned to its values before the storm on 10 April 2010 around 03.00UT.

[37] AU and AL indices (Figure 2d) exhibited 3 main maximum values, on 5 April 2010 at around 08:26 UT (350 nT for AL and 2000nT for AU), on 6 April around 01:26 UT (350nT for AL and 1000 nT for AU) and on 7 April 2010 around 17.30 UT (350nT for AL and 1500 NT for AU).

[38] At the SSC time, the increase of the solar wind component V from 500 km/s to 800 km/s (Figure 2a) is associated to an increase of the southward IMF Bz component (19 nT) (Figure 2b). At the SSC time we can also observe the increase of Dst amplitude which reached ∼35nT, followed by a decrease ∼ −50nT (Figure 2c) and increases of AL and AU indices. All these observations are the effects of the shock associated with the coronal mass ejection of 3 April 2010 which reached the Earth on 5 April 2010 [*Möstl et al.*, 2010].

[39] The image of SOHO Extreme UV Telescope, Space weather Web site predicted "a solar wind stream indicating a coronal hole that should reach Earth on 6–7 April" (http://spaceweather.com/archive.php?view=1&day=06&month=04&year=2010 updated on 23 November 2011.)

[40] On 6 April, the increase of the southward component of the IMF Bz, reaching −5 nT (Figure 2b) during one day, is associated to a decrease of the Dst ∼ −80 nT and disturbed values of AL and AU indices.

[41] Figure 3 illustrates the time variation of the ionospheric and magnetic data during the quiet magnetic period and geomagnetic storm from 3 to 10 April 2010. From top to bottom are drawn the vTEC (Figure 3a), the magnetic variations (Figure 3b), the ionospheric disturbance Diono (Figure 3c) and the convection electric field (Figure 3d).

[42] Figure 3a shows the time variation of the vTEC component observed (full lines) superimposed to the vTEC quiet reference based on the very quietest magnetic days of April 2010 ⟨vTECquiet⟩. We can note that on the magnetic quiet days of 3–10 April (see Table 2), the vTEC observed and the ⟨vTECquiet⟩matched very well: they reached the maximum value of 30 tecu around 12.00 UT. During the initial phase, on 5 April, vTEC observed is higher than the ⟨vTECquiet⟩, 25% more. The vTEC observed reached the maximum value of 40 tecu on 5 April 2010. During the recovery phase 6–7 April, vTEC observed is lower than ⟨vTECquiet⟩, 25% less. The observed vTEC reached the values 20 tecu compare to 30 tecu for the ⟨vTECquiet⟩. At the end of the recovery phase, vTEC observed on 8, 9, and 10 April exhibits roughly the same amplitude as the ⟨vTECquiet⟩, except at 12:00UT on 9 April.

[43] In Figure 3b, the ΔH component of the Earth's magnetic field measured at Aswan (full line) is superimposed on the quiet reference level ⟨ΔHquiet⟩ (dashed line), and the dashed line exhibits the well-known regular pattern of the Sq for a station located below the focus in the northern hemisphere. We can note that on the quiet days 3 and 10 April, the observed ΔH and the average ⟨ΔHquiet⟩ matched very well. They reached the maximum values of 80nT. We must recall here that we used the raw data of the MAGDAS network. It is clear that the real ΔH is around 30 nT if we withdraw the midnight zero level around 50nT, in the following we will use the raw data. On 4 April 2010, the day before the storm the observed ΔH is higher than the ⟨ΔHquiet⟩, 40% more. During the initial phase of the storm, on 5 April, ΔH reached the maximum value of 105 nT at 08:26 UT, and then suddenly decreases to a value of −15 nT at 10:00 UT, to increase again and reach the value of 85 nT during 3 h only from 08:26 UT to 12:00UT. During the recovery phase 6–7 April, we can observe the reversal of the observed ΔH compare to regular Sq pattern ⟨ΔHquiet⟩. In order to understand the ionospheric electric current disturbance Diono we need to extract from the observed ΔH the effect of the magnetospheric current and of the regular current S_R (see the paragraph data processing).

[44] Figure 3c illustrates the time variation of Diono deduced from the observed ΔH. Diono exhibits an irregular pattern with different minima on the dayside with superimposed oscillations or 1 or 2 h. We must recall here that in this case ΔH the correction of the night zero level is made though the computation (see data processing). During the recovery phase, on 6, 7, and 8 April the amplitude of the minima are respectively −85nT, −45nT and −25nT. All these minima occurred at 11:30 UT, 11:00 UT and 11:30 UT respectively. In Figure 3d, during the initial phase of the storm on 5 April 2010, IEF ($-V_x \times B_z$) reached the maximum value 10,000 mV/M at around 08:26 UT and minimum value −15,000 mV/M at around 12:00UT.

3.2. Results and Discussion

[45] In Figure 3, 3 and 10 April 2010 are magnetic quiet days (Figure 3). On these days the observed vTEC follows very well the mean ⟨vTECquiet⟩ and the observed ΔH follows also the mean ⟨ΔHquiet⟩.

[46] On 4 April, before the shock event of 5 April, the ΔH variation exhibits the regular Sq pattern with a very strong amplitude, this observation prior to the CME impact cannot be interpreted as due to the CME. This large variation can be explained by atmospheric sources.

[47] The CME impacts the Earth on 5 April at 08.25. During the beginning of the main phase of the storm, from 08.25 to 12.00, the Bz is southward. The AU and Al exhibit maxima (500nT and 2000nT). We can observe an increase of the interplanetary electric field (IEF) associated with an increase in TEC and Diono at low latitudes. These observations can be interpreted as the effect of the prompt penetration of magnetospheric convection electric field [*Vasyliunas*, 1970]. Indeed this physical process affects simultaneously high and low latitudes When Bz is northward at 12.00, we can observe a strong decrease of the TEC and ΔH. But at that time another physical process, the ionospheric disturbance dynamo [*Blanc and Richmond*, 1980] can also be invoked to explain the observations. Indeed, several hours is

the time delay needed by the ionospheric disturbance dynamo to reach low latitudes. Many observations of the ionospheric disturbance dynamo were made before this study.

[48] At low latitudes the electric fields play a key role in the dynamics of the ionosphere, in our case it causes the positive ionospheric storm in the initial phase, whereas neutral winds and composition also play an important role at low latitudes after several hours [*Fejer et al.*, 1983; *Sastri*, 1988; *Yizengaw et al.*, 2005]. During the main phase, a combination of two mechanisms could be responsible for this observed positive phase.

[49] An eastward electric field will cause increases in the midlatitude ionospheric electron density by moving the plasma particles upward, and decreases in the equatorial ionospheric electron density by strengthening the fountain effect [*Yizengaw et al.*, 2005]. The daytime poleward wind was reduced or even reversed during the storm, which may also contribute to the occurrence of the positive storm. The eastward prompt-penetration electric field associated with the southward IMF Bz at around 13:30 UT increases the regular daytime eastward dynamo electric field .Thus, it is clear that the peaks and crests of ionization are related to the changes in the interplanetary and geomagnetic conditions on 5 April. This implies that the storm on 5 April has a very strong effect on the ionospheric response over the Egypt.

[50] On 6 April 2010, there is long time duration of southward Bz (Figure 2b), westward IEF (Figure 3d), and strong westward electrojet (Figure 2d) . We observed a TEC and Diono (Figures 3a and 3c) smaller than the regular mean value, this was previously found by *Vijayakrishnan et al.* [2008] who observed a decrease of foF2 as due to a westward electric field related to a southward Bz. On 6 April, both prompt penetration of electric fields and ionospheric disturbance dynamo are acting at low latitude. *Buonsanto* [1999] and *Pi et al.* [2000] studied the prompt penetration of the magnetospheric convection with the radar chain at 75°W in a number of experiments.

[51] During the recovery phase we observed always the same feature, three minima of Diono (Figure 3c) on 6, 7, and 8 April. This is the signature of the ionospheric disturbance dynamo [*Blanc and Richmond*, 1980] which causes at low latitudes a reverse Sq current system and the depletion of vTEC . The perturbation of Diono main pattern is related to the DP2 current system [*Nishida*, 1968] and Ddyn [*Le Huy and Amory-Mazaudier*, 2005]. We can see the superposition of DP2 (oscillations of 1 or 2 h) and Ddyn: a strong minimum around 12.00. It is the first time that we can observe several days of the ionospheric disturbance dynamo effect at low latitudes, associated to high speed solar wind streams generated by a coronal hole.

[52] *Danilov and Lastovicka* [2001], *Vijayakrishnan et al.* [2008], and *Yizengaw et al.* [2005] observed the signature of the electric field on vTEC due to the storm wind generated by the Joule heating: they found a negative effect of the ionospheric storm especially during the storm recovery phase.

4. Conclusion

[53] 1. The GPS TEC measurements from Helwan station shows that the very severe magnetic storm created both enhancement and depletion of TEC relative to quiet time variation, i.e., both positive phases and negative of the storm, respectively, followed by a strong nighttime enhancement (Figure 3a).

[54] 2. The most dominant effect on the magneto–ionospheric disturbance is the ionospheric dynamo during this event.

[55] 3. The positive phase of the ionospheric storm appears after 3 h as a response to the magnetic storm.

[56] 4. During spring season, the penetration electric field and ionospheric dynamo combine to cause a positive phase corresponding to the main phase of the storm.

[57] 5. The negative phase is due to the day time ionospheric dynamo during the effect of the long period of coronal hole and Bz south corresponding to the recovery phase of the storm.

[58] 6. Clearly, pre-reversal (night enhancement) phenomena were observed at sunset.

[59] 7. On 4 April 2010 (Am = 25), we cannot explain the peak of the daily H magnetic component. It is increasing more than that of mean value of most quiet H. The source phenomena is probably atmospheric.

[60] 8. Efforts must be concentrated on the ionospheric disturbance dynamo magnetic signature at equatorial and low latitudes in order to better understand the circulation of the various currents generated during this type of long period geomagnetic storms.

References

Abdu, M. A., J. H. Sastri, J. MacDougall, I. S. Batista, and J. H. A. Sobral (1997), Equatorial disturbance dynamo electric field longitudinal structure and spread F: A case study from GUARA/EITS campaigns, *Geophys. Res. Lett.*, 24, 1707–1710, doi:10.1029/97GL01465.

Blanc, M., and A. D. Richmond (1980), The ionospheric disturbance dynamo, *J. Geophys. Res.*, 85(A4), 1669–1686, doi:10.1029/JA085iA04p01669.

Buonsanto, M. J. (1999), Ionospheric storms—A review, *Space Sci. Rev.*, 88, 563–601, doi:10.1023/A:1005107532631.

Cole, K. D. (1966), Magnetic storms and associated phenomena, *Space Sci. Rev.*, 5, 699–770, doi:10.1007/BF00173103.

Connors, M., C. T. Russell, and V. Angelopoulos (2011), Magnetic flux transfer in the 5 April 2010 Galaxy 15 substorm: An unprecedented observation, *Ann. Geophys.*, 29, 619–622, doi:10.5194/angeo-29-619-2011.

Danilov, A. D., and J. Lastovicka (2001), Effects of geomagnetic storms on the ionosphere and atmosphere, *Int. J. Geomagn. Aeron.*, 2(3), 209–224.

Fambitakoye, O., M. Menvielle, and C. Mazaudier (1990), Global disturbance of the transient magnetic field associated with thermospheric storm winds on March 23, 1979, *J. Geophys. Res.*, 95, 15,209–15,218, doi:10.1029/JA095iA09p15209.

Fejer, B. G., and L. Scherliess (1995), Time dependent response of equatorial ionospheric electric fields to magnetospheric disturbances, *Geophys. Res. Lett.*, 22(7), 851–854, doi:10.1029/95GL00390.

Fejer, B. G., M. F. Larsen, and D. T. Farley (1983), Equatorial disturbance dynamo electric fields, *Geophys. Res. Lett.*, *10*, 537–540, doi:10.1029/GL010i007p00537.

Fukushima, N., and Y. Kamide (1973), Partial ring current models for worldwide geomagnetic disturbances, *Rev. Geophys.*, *11*, 795–853, doi:10.1029/RG011i004p00795.

Groves, K., et al. (1997), Equatorial scintillation and systems support, *Radio Sci.*, *32*, 2047–2064, doi:10.1029/97RS00836.

Jones, K. L. (1971), Storm time variation of the *F2* layer electron concentration, *J. Atmos. Terr. Phys.*, *33*, 379–389, doi:10.1016/0021-9169(71)90143-7.

Jones, K. L., and H. Rishbeth (1971), The origin of storm increases of midlatitude *F*-layer electron concentration, *J. Atmos. Terr. Phys.*, *33*, 391–401, doi:10.1016/0021-9169(71)90144-9.

Kikuchi, T., H. Luehr, T. Kitamura, O. Saka, and K. Schlegel (1996), Direct penetration of the polar electric field to the equator during a *DP2* event as detected by the auroral and equatorial magnetometer chains and the EISCAT radar, *J. Geophys. Res.*, *101*, 17,161–17,173, doi:10.1029/96JA01299.

Kobéa, A. T., C. Amory-Mazaudier, J.-M. Do, H. Lürh, J. Vassal, E. Houngninou, E. Blanc, and J.-J. Curto (1998), Equatorial electrojet as part of a global current system: Data, *Ann. Geophys.*, *16*, 698–710, doi:10.1007/s00585-998-0698-1.

Kobéa, A. T., A. D. Richmond, B. A. Emery, C. Peymirat, H. Lürh, T. Moretto, M. Hairston, and C. Amory (2000), Electrodynamic coupling between high and low latitudes: Observations on May, 27, 1993, *J. Geophys. Res.*, *105*(A10), 22,979–22,989, doi:10.1029/2000JA000058.

Le Huy, M., and C. Amory-Mazaudier (2005), Magnetic signature of the ionospheric disturbance dynamo at equatorial latitudes: "D$_{dyn}$," *J. Geophys. Res.*, *110*, A10301, doi:10.1029/2004JA010578.

Le Huy, M., and C. Amory-Mazaudier (2008), Planetary magnetic signature of the storm wind disturbance dynamo currents: D_{dyn}, *J. Geophys. Res.*, *113*, A02312, doi:10.1029/2007JA012686.

Maeda, G., and K. Yumoto (2009), Progress report on the deployment of MAGDAS, *Earth Moon Planets*, *104*, 271–276, doi:10.1007/s11038-008-9284-5.

Mayaud, P. N. (1980), *Derivation, Meaning, and Use of Geomagnetic Indices*, Geophys. Monogr. Ser., vol. 22, 154 pp., AGU, Washington, D. C.

Mazaudier, C. (1985), Electric currents above Saint-Santin: 3. A preliminary study of disturbances: June 6, 1978; March 22, 1979; March 23, 1979, *J. Geophys. Res.*, *90*(A2), 1355–1366, doi:10.1029/JA090iA02p01355.

Mazaudier, C., and R. Bernard (1985), Saint-Santin radar observations of lower thermospheric storms, *J. Geophys. Res.*, *90*, 2885–2895, doi:10.1029/JA090iA03p02885.

Mazaudier, C., and S. V. Venkateswaran (1990), Delayed ionospheric effects of the geomagnetic storms of March 22, 1979 studied by the sixth Coordinated Data Analysis Workshop (CDAW-6), *Ann. Geophys.*, *8*, 511–518.

Mazaudier, C., R. Bernard, and S. V. Venkateswaran (1985), Correction to "Saint-Santin radar observations of lower thermospheric storms," *J. Geophys. Res.*, *90*, 6685–6686, doi:10.1029/JA090iA07p06685.

Mene, N. M., A. T. Kobéa, O. K. Obrou, K. Z. Zaka, K. Boka, C. Amory-Mazaudier, and P. Assamoi (2011), Statistical study of the DP2 enhancement at the dayside dip-equator compared to low latitudes, *Ann. Geophys.*, *29*, 2225–2233, doi:10.5194/angeo-29-2225-2011.

Menvielle, M., H. McCreadie, and C. Barton (2009), *IAGA Guide for Geomagnetic Indices Derived From Earth Surface Data*, IAGA, Paris.

Möstl, C., M. Temmer, T. Rollett, C. J. Farrugia, Y. Liu, A. M. Veronig, M. Leitner, A. B. Galvin, and H. K. Biernat (2010), STEREO and Wind observations of a fast ICME flank triggering a prolonged geomagnetic storm on 5–7 April 2010, *Geophys. Res. Lett.*, *37*, L24103, doi:10.1029/2010GL045175.

Nishida, A. (1968), Geomagnetic D$_p$ 2 fluctuations and associated magnetospheric phenomena, *J. Geophys. Res.*, *73*, 1795–1803, doi:10.1029/JA073i005p01795.

Nishida, A., N. Iwasaki, and N. T. Nagata (1966), The origin of fluctuations in the equatorial electrojet: A new type of geomagnetic variation, *Ann. Geophys.*, *22*, 478–484.

Peymirat, C., A. D. Richmond, and A. T. Kobea (2000), Electrodynamic coupling of high and low latitudes: Simulations of shielding/overshielding effects, *J. Geophys. Res.*, *105*(A10), 22,991–23,003, doi:10.1029/2000JA000057.

Pi, X., M. Mendillo, W. J. Hughes, M. J. Buonsanto, D. P. Sipler, J. Kelly, Q. Zhou, G. Lu, and T. J. Hughes (2000), Dynamical effects of geomagnetic storms and substorms in the middle-latitude ionosphere: An observational campaign, *J. Geophys. Res.*, *105*, 7403–7417, doi:10.1029/1999JA900460.

Richmond, A. D., and S. Matsushita (1975), Thermospheric response to a magnetic substorm, *J. Geophys. Res.*, *80*(19), 2839–2850, doi:10.1029/JA080i019p02839.

Richmond, A., and R. G. Roble (1979), Dynamic effects of aurora generated gravity waves on the mid-latitude ionosphere, *J. Atmos. Terr. Phys.*, *41*, 841–852, doi:10.1016/0021-9169(79)90127-2.

Richmond, A. D., C. Peymirat, and R. G. Roble (2003), Long-lasting disturbances in the equatorial ionospheric electric field simulated with a coupled magnetosphere-ionosphere-thermosphere model, *J. Geophys. Res.*, *108*(A3), 1118, doi:10.1029/2002JA009758.

Rostoker, G. (1969), Classification of polar magnetic disturbances, *J. Geophys. Res.*, *74*(21), 5161–5168, doi:10.1029/JA074i021p05161.

Sabaka, T. J., N. Olsen, and M. E. Purucker (2004), Extending comprehensive models of the Earth magnetic field with Oersted and Champ data, *Geophys. J. Int.*, *159*, 521–547, doi:10.1111/j.1365-246X.2004.02421.x.

Sastri, H. (1988), Equatorial electric field of ionospheric disturbance dynamo origin, *Ann. Geophys.*, *6*, 635–642.

Senior, C., and M. Blanc (1984), On the control of the magnetospheric convection by the spatial distribution of ionospheric conductivities, *J. Geophys. Res.*, *89*, 261–284, doi:10.1029/JA089iA01p00261

Spiro, R. W., R. A. Wolf, and B. G. Fejer (1988), Penetration of high latitude electric field effects to low latitudes during the SUNDIAL 1984, *Ann. Geophys.*, *6*, 39–50.

Testud, J., and G. Vasseur (1969), Ondes de gravit'e dans la thermosph`ere, *Ann. Geophys.*, *25*, 525–546.

Vasyliunas, V. M. (1970), Mathematical models of magnetospheric convection and its coupling to the ionosphere, in *Particles and Fields in the Magnetosphere*, edited by M. McCormac, pp. 60–71, Springer, New York, doi:10.1007/978-94-010-3284-1_6.

Vijayakrishnan, M. V., C. V. Sreehari, S. Tiju Joseph Mathew, and R. Prabhakaran Nayar (2008), Influence of IMF B_z on the variability of the minimum value of f_o-F2, *Indian J. Radio Space Phys.*, *37*, 46–50.

Volland, H. (1979), Magnetospheric electric fields and currents and their influence on large scale thermospheric circulation and composition, *J. Atmos. Terr. Phys.*, *41*, 853–866, doi:10.1016/0021-9169(79)90128-4.

Yizengaw, E., P. L. Dyson, E. A. Essex, and M. B. Moldwin (2005), Ionosphere dynamics over the Southern Hemisphere during the 31 March 2001 severe magnetic storm using multi-instrument measurement data, *Ann. Geophys.*, *23*, 707–721, doi:10.5194/angeo-23-707-2005.

Zaka, K. Z., A. T. Kobéa, P. Assamoi, O. K. Obrou, V. Doumbia, K. Boka, J.-P. Adohi, and N. M. Mene (2009), Latitudinal profiles of the ionospheric disturbance dynamo magnetic signature: Comparison with the DP2 magnetic disturbance, *Ann. Geophys.*, *27*, 3523–3536, doi:10.5194/angeo-27-3523-2009.

Zaka, K. Z., et al. (2010a), Simulation of electric field and current during the 11 June 1993 disturbance dynamo event: Comparison with the observations, *J. Geophys. Res.*, *115*, A11307, doi:10.1029/2010JA015417.

Zaka, K. Z., et al. (2010b), Correction to "Simulation of electric field and current during the 11 June 1993 disturbance dynamo event: Comparison with the observations," *J. Geophys. Res.*, *115*, A12314, doi:10.1029/2010JA016292.